



1 **Insights on the spatial distribution of global, national and sub-national GHG emissions**  
2 **in EDGARv8.0**

3 **Authors:** Monica Crippa<sup>2</sup>, Diego Guizzardi<sup>1</sup>, Federico Pagani<sup>2</sup>, Marcello Schiavina<sup>6</sup>, Michele  
4 Melchiorri<sup>1</sup>, Enrico Pisoni<sup>1</sup>, Francesco Graziosi<sup>1</sup>, Marilena Muntean<sup>1</sup>, Joachim Maes<sup>5</sup>, Lewis  
5 Dijkstra<sup>1,5</sup>, Martin Van Damme<sup>3,4</sup>, Lieven Clarisse<sup>3</sup>, Pierre Coheur<sup>3</sup>

6

7 <sup>1</sup>European Commission, Joint Research Centre (JRC), Ispra, Italy

8 <sup>2</sup>Unisystems S.A., Milan, Italy

9 <sup>3</sup>Spectroscopy, Quantum Chemistry and Atmospheric Remote Sensing (SQUARES),  
10 Université libre de Bruxelles (ULB), Brussels, Belgium

11 <sup>4</sup>Royal Belgian Institute for Space Aeronomy (BIRA-IASB), Brussels, Belgium

12 <sup>5</sup>European Commission, Directorate-General for Regional and Urban Policy, Brussels

13 <sup>6</sup>NTT DATA, Rue de Spa, 8, 1000 Bruxelles

14 Correspondence: enrico.pisoni@ec.europa.eu

15 **Abstract**

16 Knowing where emissions occur is essential for planning effective emission reduction  
17 measures and for atmospheric modelling. Emission inventories are typically compiled at  
18 national level and provide sector-specific emission estimates. Disaggregating national  
19 emissions on high-resolution grids requires spatial proxies that contain information on the  
20 location of different emission sources (e.g. point sources, linear and area sources). Knowing  
21 the correct allocation of emissions from point sources is essential to avoid the misallocating  
22 high emission levels. However, gathering information on point sources covering the entire  
23 globe and a wide temporal domain (1970 to present) is challenging due to limited data  
24 availability, accuracy of the reporting and completeness of data. The latest spatial proxies  
25 developed as part of the Emissions Database for Global Atmospheric Research (EDGARv8.0)  
26 provide the user with the possibility to work with different geographical details using a  
27 consistently developed GHG emissions database. A key novelty of EDGARv8.0 is the  
28 possibility to analyse sub-national GHG emissions over the European domain, but also over  
29 the US, China, India and main world countries. The relevance of using updated spatial  
30 information is assessed on the basis of regional case studies. The data can be accessed at  
31 <https://doi.org/10.2905/b54d8149-2864-4fb9-96b9-5fd3a020c224> specific for EDGARv8.0  
32 (Crippa, 2023a) and [doi:10.2905/D67EEDA8-C03E-4421-95D0-0ADC460B9658](https://doi.org/10.2905/D67EEDA8-C03E-4421-95D0-0ADC460B9658) for the sub-  
33 national dataset (Crippa et al., 2023b).

34 **1 Introduction**

35 Knowing where emissions happen is essential to support the design of effective mitigation  
36 actions and for atmospheric modelling purposes. Emission inventories are typically developed  
37 at national level and provide sector-specific emission estimates. In order to disaggregate  
38 national emissions over high-resolution grids, information on the location of the different  
39 emission sources (e.g. point, linear and area sources) must be collected and ‘spatial proxies’  
40 should be developed and applied to national sector specific emission totals to downscale them  
41 over gridmaps. The Emissions Database for Global Atmospheric Research (EDGAR) provides  
42 global greenhouse gas (GHG) and air pollutant emissions over the global gridmap at 0.1x0.1



43 degree resolution, although the resolution of the underlying spatial information used to  
44 downscale national totals may be higher (down to few hundred meters resolution). The  
45 development and maintenance of the EDGAR gridmaps is essential since several regional and  
46 global databases rely on the EDGAR emission gridmaps to weight national inventories. This  
47 is the case of the Community Emissions Data System (CEDS) (Feng et al., 2020; Hoesly et al.,  
48 2018) or the EMEP Centre on Emission Inventories and Projections (CEIP) to support EU  
49 Member States in their official gridded emission reporting requirements (CEIP, 2021). This  
50 work is an update of previous EDGAR publications dealing with spatial data (Janssens-  
51 Maenhout et al., 2019; Crippa et al., 2021), and describes all the new developments for the  
52 spatialisation of the emissions from EDGARv8.0 onwards.

53 Knowing the correct allocation of point source emissions is essential to avoid the misplacement  
54 of high emission levels. However, gathering information on point sources covering the entire  
55 globe and a wide temporal domain (1970 to present) is challenging due to limited data  
56 availability, accuracy in the reporting (real location vs. legal site, etc.) and completeness of  
57 data. The latest spatial proxies developed within EDGAR will be presented in this work,  
58 focusing on high emitting sectors such as power plant and industrial activities, but also on more  
59 distributed sources such as residential activities. High resolution spatial information has been  
60 gathered at the global level combining Global Energy Monitor data, official registries and  
61 satellite retrievals. The relevance of using updated spatial information is also assessed with  
62 regional case studies.

63 The purpose of this publication is describing the EDGARv8.0 GHG gridded emission datasets,  
64 focusing on the updates of the spatial proxies included in this data release. The analysis of  
65 EDGARv8.0 emission time series (European Union, 2023; IEA-EDGAR CO<sub>2</sub>, 2023) and the  
66 methodology behind emission calculations is available in Crippa et al. (2023c).

67 Main novelties of this work are i) update of emission point sources using global datasets (e.g.  
68 Global Energy Monitor), ii) development of a gap-filling method for non-population based  
69 sources using built-up surface information for non-residential areas from the Global Human  
70 Settlements Layer (GHSL), iii) update of population based proxies using the latest GHSL data  
71 including a weight for meteorological dependence of heating needs, and v) update of  
72 international ship tracks and weights by vessel type. In addition, information at sub-national  
73 level (e.g. for Europe at NUTS2 level) is included when developing the new spatial proxies of  
74 EDGAR, thus allowing a more accurate allocation and analysis of sub-national emissions. The  
75 EDGARv8.0 GHG global emission maps can be accessed at [doi:10.2905/D67EEDA8-C03E-4421-95D0-0ADC460B9658](https://doi.org/10.2905/D67EEDA8-C03E-4421-95D0-0ADC460B9658)  
76 for the subnational emissions, and at [doi: 10.2905/B54d8149-2864-4FB9-96B9-5FD3A020C224](https://doi.org/10.2905/B54d8149-2864-4FB9-96B9-5FD3A020C224)  
77 for v8.0 for the emission gridmaps at 0.1x0.1 degree resolution.

## 78 **2 Overview on the methodology and data sources used for updating spatial information** 79 **in EDGAR**

80 Bottom-up global inventories, such as EDGAR, compute emissions for each sector, pollutant  
81 and year at country level making use of international statistics and official guidelines for  
82 emission computation (Janssens-Maenhout et al., 2019; Crippa et al., 2018). However,  
83 atmospheric modellers, policy makers, local authorities and scientists may need to analyse  
84 spatially distributed emissions than country level data. Therefore, annual country specific  
85 emissions are distributed over the globe making use of spatial information, representing either  
86 the exact location of points sources (e.g. power plants, industrial facilities, etc.), or linear tracks



87 (e.g. road network, ship and airplane tracks, etc.), or area sources (e.g. populated areas,  
88 industrial areas, etc.). Within the EDGAR database, over 130 proxy datasets (f) varying over  
89 time are developed to weight the contribution of sector specific emissions ( $EM_{i,j,k}$ ) of each  
90 country (C) and pollutant (x) over time (t) to each gridcell ( $em_{i,j,k}$ ) at  $0.1^\circ \times 0.1^\circ$  resolution (about  
91 10km at the equator) spatial resolution (WGS84, EPSG:4326), with the Heaviside function,  
92 equalling 1 when the grid cell belongs to the country area, accordingly with the following  
93 formula:

$$94 \quad em_{i,j,k}(lon, lat, t, x) = EM_{i,j,k}(C, t, x) \cdot \frac{f_{i,j,k}(lon, lat, t)}{\sum_{lon, lat} (f_{i,j,k}(lon, lat, t) \cdot H_{i,j}(C, lon, lat))}$$

95

96 Where

97  $H_{i,j}(C, lon, lat)$  = fraction/weight of gridcell within C,

98 i=sector,

99 j=fuel,

100 k=technology.

101 Table 1 summarises the data sources and the methodology used to update spatial information  
102 for each emitting sector in the EDGAR database, highlighting the most relevant and latest  
103 updates compared to previous EDGAR data releases. These updates apply from EDGARv8.0  
104 onwards. Being a global database of emissions, the spatial data sources used are typically  
105 developed at the global level (e.g. satellite based retrievals, etc.), although often relying on  
106 national data collections (e.g. national point source information reported to fulfill legal  
107 requirements). Therefore, the same data sources may be used by other inventory developers to  
108 update their spatial disaggregation of the emissions. In the following sections, a detailed  
109 description on the data sources and approach used for updating each emission sector is  
110 provided, distinguishing between point sources, area sources and linear sources. For all sectors  
111 not subjected to a recent revision in the EDGAR database, we recommend the reader to rely on  
112 the overview Table S1 and there references therein.

113 A key methodological advancement in the EDGAR gridding system is also represented by the  
114 inclusion of the correct sub-national information for each spatial data and in particular for each  
115 point source. This implies attaching to each point not only its exact location expressed in  
116 longitude and latitude, but also the related NUTS2 (Nomenclature of territorial units for  
117 statistics) code (EUROSTAT, 2021) for Europe or the Global ADMInistrative layer at level 1  
118 (GADM version 4.1). The choice of including NUTS2 rather than NUTS3 information aims at  
119 enhancing the capability of a global database such as EDGAR to represent sub-national  
120 regional emissions in support of the development of regional policies (e.g. EU Cohesion  
121 Reports (European Commission, 2022) or the 2040 Climate Impact Assessment), while  
122 compromising with the global dimension of the database. In fact, the attribution of subnational  
123 details is not only developed with an EU oriented focus, but also it allows approaching for  
124 example the Unites States, China and India not anymore at national-level administrative  
125 boundary, but providing emissions on each US state, each Chinese province and Indian state  
126 Moving towards province or city scale dimension starting from national emissions is not only



127 subjected to the association of e.g. point sources to NUTS3 level but also relying on more  
128 disaggregated statistics. Therefore, considering the current purposes of EDGAR the NUTS2  
129 level represent the right balance between accuracy of the final emissions and downscaling of  
130 national totals. The relevance of including not only country specific details, but also sub-  
131 regional information is essential when doing emission data extraction at sub-national level,  
132 thus avoiding border issues. Some inventory compilers (Kuenen et al., 2022), report point  
133 source information just as points without distributing them over a gridmap with a certain  
134 resolution. This approach is accurate since it provides the exact geographical coordinates of  
135 individual facilities; however, it does not reduce data extraction issues, since the allocation of  
136 a specific point to a certain gridcell cell may fall between the borders of e.g. two regions.  
137 Another challenge that we address with this new gridding approach is related with the  
138 harmonization of national and sub-national data. Local and regional inventories are often  
139 developed independently, therefore, undermining the possibility to collate together sub-  
140 national emissions to retrieve the national values. The challenge of using different and not  
141 coherent databases is overtaken by the EDGAR database, being able to consistently work both  
142 at the national and regional level, thus offering the user the possibility to work across different  
143 geographical scales. In the results section, case studies on sub-national emissions are presented  
144 for the EU, US, China and India.

### 145 **3 Point sources of emissions**

146 Gathering information on point sources covering the globe and spanning a wide temporal  
147 domain (1970-nowadays) is challenging due to the limited data availability, accuracy and  
148 completeness in the reporting (real plant location vs. legal site, etc.). The correct location of  
149 point sources is essential since they are often super emitters (e.g. power plants for CO<sub>2</sub>  
150 emissions). In EDGARv8.0, the location of main industrial point sources (e.g. power plants,  
151 iron and steel industries and other plants, coal mines, venting and flaring activities, etc.), which  
152 contribute for around half of global CO<sub>2</sub> emissions, has been updated using state of the art  
153 information making use of global databases, such as the Global Gas/Coal Plant Tracker of the  
154 Global Energy Monitor. A complete overview of the data sources and updates included in  
155 EDGARv8 is provided in Table 1. In the following, we will describe sector by sector how the  
156 most up to date spatial data on point sources have been collected and implemented in the  
157 EDGAR database to downscale national emissions over the global gridmap.

#### 158 **3.1 Power plants**

159 Power plants represent a major source of fossil CO<sub>2</sub> and GHG emissions globally, contributing  
160 nowadays for around 38% and 18%, respectively, to the corresponding global totals (Crippa et  
161 al., 2023c). It is therefore of utmost importance including the latest available information to  
162 correctly allocate these emissions at the global level and understand their evolution over time,  
163 in order to design and implement adequate emission mitigation measures. In EDGARv8.0, fuel  
164 specific spatial proxies have been developed using data from the Global Coal and Gas Plant  
165 Tracker of the Global Energy Monitor (for coal and gas) (Global Energy Monitor, 2022d, a),  
166 the Global Power Plant Database v1.3.0 (World Resources Institute, 2018; WRI, 2021) for oil  
167 and biofuels, CARMAv3.0 for autoproducers (i.e. plants and industries producing power for  
168 their own use). In addition, information on autoproducers and biofuel fired power plants in  
169 Europe has been integrated using the European Pollutant Release and Transfer Register  
170 (EPRTRv18) (EPRTR, 2020). For the US domain, the location of fossil fuel fired power plants

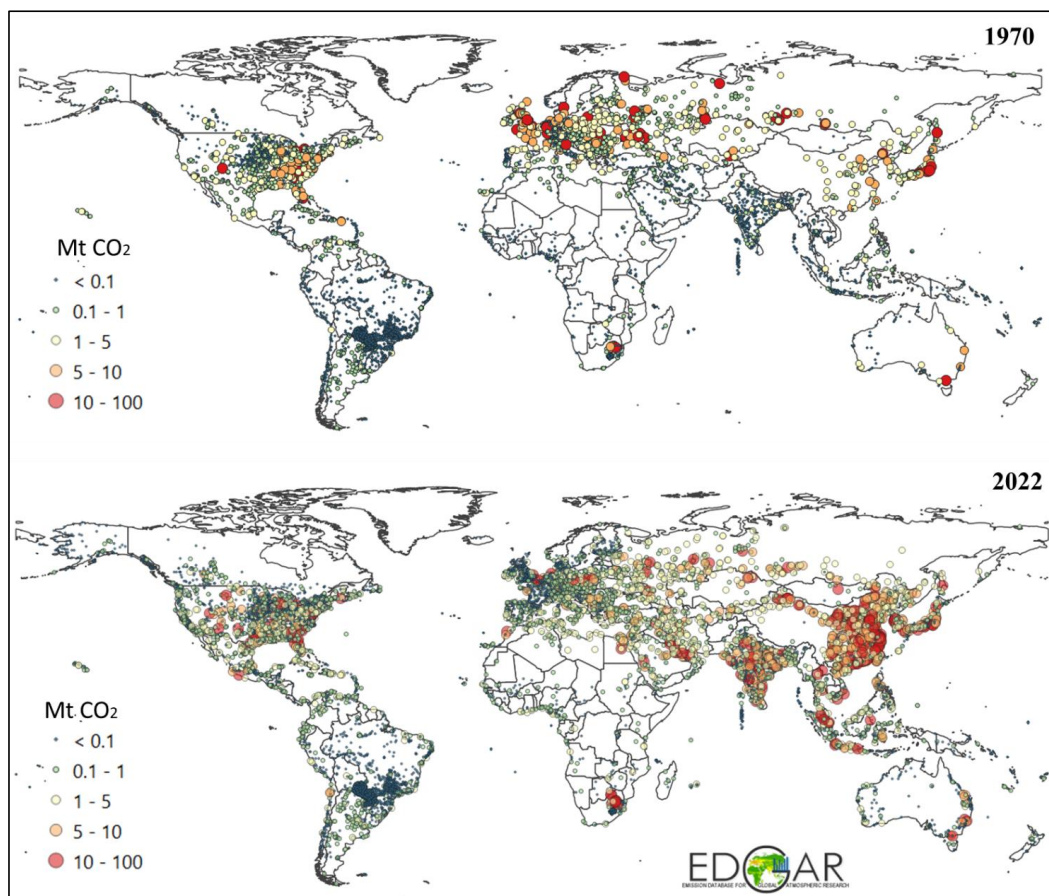


171 is taken from the US Energy Information Administration (US EIA, 2022b) as they represent  
172 the most updated source for the US. The time frame covered by the new power plant spatial  
173 proxy datasets developed in EDGARv8.0 is 1970-2022, which includes for each plant  
174 information on opening and closing years (also beyond 2022 for recently built power plants),  
175 capacity, main fuel type, etc. When only partial information is available for the years of  
176 operations, assumptions on the typical lifetime of power plants is assumed (e.g. 40 years). The  
177 capacity of each power plant is used to relatively weight within a country the fuel specific  
178 emissions from power plants. An additional adjustment is performed over the US domain, to  
179 take into account for the different sulphur content in the fuel used in the different US states  
180 based on EIA and FERC utility surveys.

181 The Global Energy Monitor is chosen as main data source for updating power plants proxies  
182 since it relies on data from public and private data sources (including the Global Energy  
183 Observatory, CARMA, Platts World Energy Power Plant database, national-level trackers  
184 developed by environmental organisations, as well as various company and government  
185 sources). It is validated with i) government data on individual power plants, ii) country energy  
186 and resource plans, and government websites tracking coal plant permits and applications, iii)  
187 reports by state-owned and private power companies, iv) news and media reports, v) local non-  
188 governmental organizations tracking coal plants or permits. Local experts are also involved in  
189 the review of coal and gas plant data. Regular bi-annual updates of these databases also  
190 guarantee the possibility to include further updates in future EDGAR releases. As of January  
191 2019, the Global Coal Plant Tracker included exact locations for 95.3% of operating units  
192 (6411 out of 6725). Independent use and validation of the Global Coal and Gas Plant Trackers  
193 is also performed by Guevara et al. (2023). Figure S1 shows the comparison between the geo-  
194 coverage of EDGARv8.0 and the previous EDGAR spatial data for power plants, while Fig.  
195 S2 provides a view on the global coverage of power plants in EDGARv8.0 by fuel type.

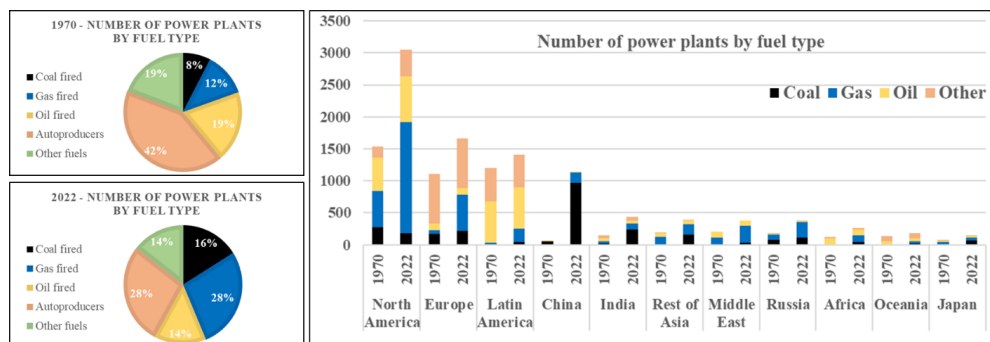
196 Figure 1 shows the global coverage and intensity of CO<sub>2</sub> emissions from fossil fuel fired power  
197 plants from EDGARv8.0 for the years 1970 and 2022. As a general trend, the number of power  
198 plants highly increased from 1970 to 2022 (see also Fig.2). The total number of power plants  
199 grew from around 8500 in 1970 to 13000 in 2022, with the sharpest increase occurring in China  
200 (4.5 times more) and North America (2 times more). However, the intensity of the emissions  
201 changed over the past 5 decades, depending on the region. As shown in Fig.2, despite the  
202 increase in the regional number of power plants, shift towards cleaner fuels is found in  
203 industrialised regions together with increased energy efficiency, which lead to stable and lower  
204 CO<sub>2</sub> emissions (e.g. 13% decrease in Europe between 1970 and 2022). On the contrary,  
205 emerging regions are characterised by significantly higher emissions in 2022 and the use of  
206 high C content fuels, such as coal. Over the past 5 decades, fossil CO<sub>2</sub> emissions from power  
207 plants increased up to 42 and 38 times in China and India, respectively. Country specific trends  
208 of CO<sub>2</sub> and GHG emissions from power plants are presented in Crippa et al. (2023c).

209



210

211 **Figure 1 – CO<sub>2</sub> emissions from fossil fuel fired power plants in 1970 and 2022 from EDGARv8.0. The size**  
 212 **of the circles is proportional to the magnitude of the emissions.**



213

214 **Figure 2 - Evolution of the total number of power plants (including fossil and bio fuels fired) from 1970 to**  
 215 **2022 by world region included in the updated EDGAR spatial proxies.**

216

217

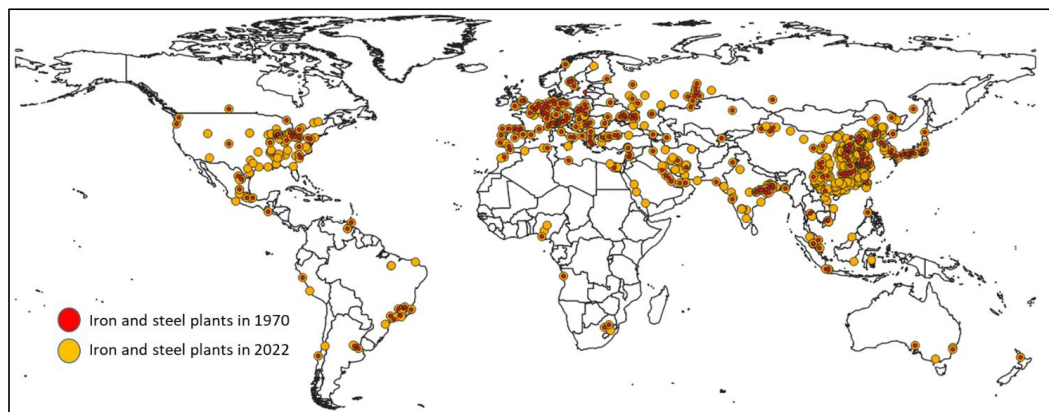


### 218 **3.2 Industrial facilities and other point sources**

219 Industrial activities cover a wide range of sectors encompassing manufacturing, the production  
220 of iron and steel, cement, glass, metals, solvents, chemicals, or fertilisers but also intensive  
221 animal farming (see section 3.4). Gathering information on industrial activities (e.g.  
222 production, capacity, location of the facilities, etc.) at the global level is challenging, also due  
223 to confidentiality and data protection issues. For this reason, we partly focussed on the update  
224 of information on industrial point sources (when available), while we improved the gap-filling  
225 method for all industrial activities in case of incomplete or missing data (as discussed in detail  
226 in Sect. 3.5). In EDGARv8.0, we included the latest European Pollutant Release and Transfer  
227 Register (EPRTRv18) locations for all industrial facilities (with the exception of power plants,  
228 iron and steel facilities and coal mines, for which dedicated spatial proxies have been developed  
229 at global level). Several manual adjustments were implemented to overcome data quality issues  
230 related with missing spatial information and inconsistencies. The analysis of the EPRTR  
231 dataset also inspired the idea of attributing only a fraction of the emissions to the reported point  
232 sources. This is also justified by the fact that industrial facilities have to report their emissions  
233 only if they fall above a certain threshold. The fraction of the emissions to be allocated to the  
234 available point sources is determined through the ratio between EPRTR emissions (typically  
235 of CO<sub>2</sub>) and the corresponding EDGAR emissions. When the ratio is 1, all emissions are  
236 allocated to the point sources; when the ratio is lower than 1, the complementary fraction is  
237 then attributed to the gap-filling grid (i.e. non-residential proxy as defined in Sect. 3.5).

238 In EDGARv8.0, we have also updated the global locations of iron and steel plants, which are  
239 among the most energy intensive industries. The Global steel plant tracker of the Global Energy  
240 Monitor (2022c) was used as data source due to its global and temporal completeness (1970-  
241 present). A map of iron and steel production plants in 1970 and 2022 is presented in Fig.3. The  
242 number of iron and steel plants increased around tenfold over the last five decades (from 77 to  
243 728) with the sharpest increase in China (fivefold), USA and India (2.7-fold).

244 Coal Mines are also a relevant source of fugitive emissions of GHGs and air pollutants (e.g.  
245 volatile organic compounds). In EDGARv8.0, we updated the information on coal mines at  
246 global level using the Global Coal Mine Tracker of the Global Energy Monitor (2022b)  
247 complemented with the Energy Information Administration data for the US (US EIA, 2022a).  
248 For countries not covered by these data sources, we relied on the previous EDGAR spatial  
249 proxies including data from the US Geological Survey (USGS, 2019). More specifically, we  
250 included information on surface and underground mines both for hard and brown coal.



251

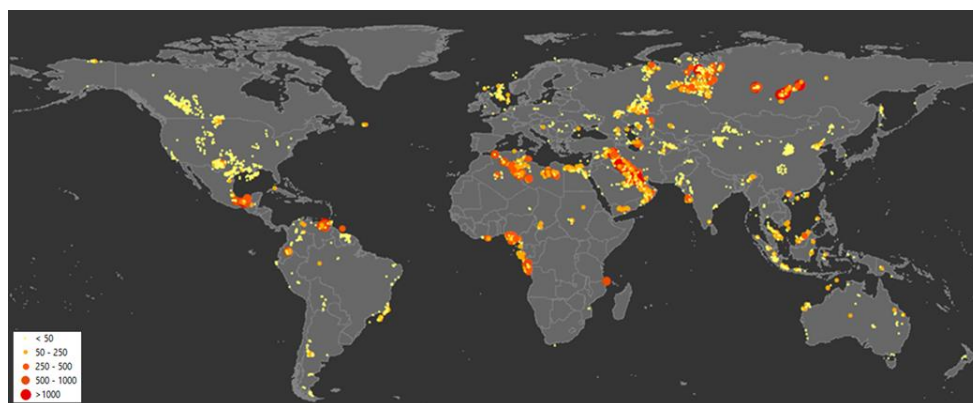
252 **Figure 3 – Global location of iron and steel plants in 1970 and 2022.**

### 253 **3.3 Venting and flaring**

254 Gas flaring is the burning of the natural gas associated with oil extraction. Although this  
255 practice is highly polluting and represents a waste of resources, it is still in place due to  
256 economic constraints and lack of appropriate legislation in several countries. Flaring takes  
257 place both as on-shore and off-shore activities and it is a source of GHG and air pollutant  
258 emissions.

259 Global CO<sub>2</sub> emissions related with flaring account for 276 Mt in 2022, of which 50% is emitted  
260 only by four countries, namely Russia (18% of the global total), Iraq (13%), Iran (12%) and  
261 Venezuela (7%). 76% of the global CO<sub>2</sub> emissions from flaring activities is produced by 10  
262 top emitting countries with individual contribution higher than 2% of the global total (including  
263 Algeria, USA; Mexico, Libya, Nigeria and China in addition to the abovementioned top 4).  
264 Although this emission source represents only 0.8% of global CO<sub>2</sub> emissions, it is particularly  
265 relevant for certain regions in the world, such as Venezuela (20% of the CO<sub>2</sub> country total),  
266 Iraq (18%), Libya (17%), Algeria (10%) and Nigeria (9%). Considering the relevance of  
267 venting emissions and the potential of control measures, it is essential to best quantify and  
268 attribute the correct georeference for this source. Flaring emissions can also be localised and  
269 quantified through space born measurements (Elvidge et al., 2017; NOAA, 2017). In  
270 EDGARv8.0, data from the World Bank Global Gas Flaring Tracker Report (2023) were used  
271 both for estimating the emissions and location of global flaring activities from 2012 till 2022.  
272 These spatial data were also used as best approximation to spatially distribute emissions from  
273 venting although the two activities may not overlap. The resulting CO<sub>2</sub> emission map in 2012  
274 and 2022 is reported in Fig. 4.



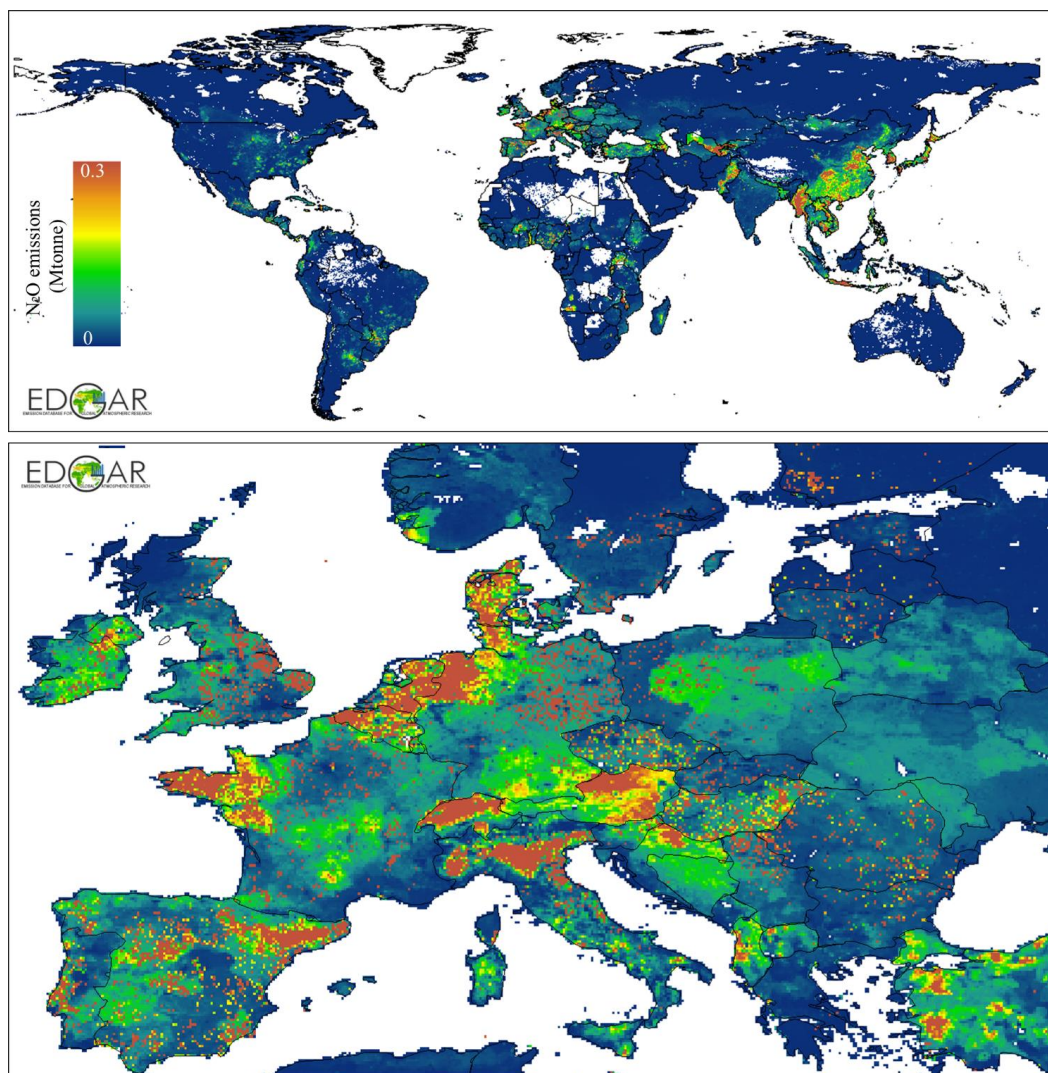


275

276 **Figure 4 – Global map of CO<sub>2</sub> emissions (kton) from flaring in 2022.**

### 277 **3.4 Intensive livestock and fertiliser industries**

278 Agriculture includes a variety of activities that are typically distributed over large areas (e.g.  
279 crop areas, animal pastures, etc.). However, several agricultural activities can be defined as  
280 hot-spots or point sources and include intensive animal farming and manure management  
281 practices. In a broader sense, we allocate to this sector also fertiliser industries which represent  
282 an important source of NH<sub>3</sub> and N<sub>2</sub>O. In EDGARv8.0, the IASI satellite-derived NH<sub>3</sub> point  
283 source database (Van Damme et al., 2018; Clarisse et al., 2019) is included to map animal  
284 farming and fertiliser production emissions with yearly information for the period 2008-2022.  
285 It includes 270 agricultural hot-spots and 251 production facilities of synthetic NH<sub>3</sub> worldwide.  
286 Since the NH<sub>3</sub> point source database includes only hot-spots we decided to allocate to these  
287 points only a fraction of the total emissions for that sector and country, while distributing the  
288 remaining fraction to livestock density maps formerly available in EDGAR. Similarly to what  
289 was done for other industries, for Europe, intensive livestock point sources were taken from  
290 EPRTRv18. Similarly, the satellite-based information on fertiliser industries was integrated in  
291 the previous EDGAR proxy for this sector. This update represents a significant improvement  
292 in representing N related hot-spots compared to former EDGAR releases (Van Damme et al.,  
293 2018), although considering the uncertainty of IASI information of around 50%. A snapshot  
294 on N<sub>2</sub>O emissions from manure management at global level and in Europe, where intensive  
295 livestock activities appear as emission hot-spots is shown in Fig. 5.



296

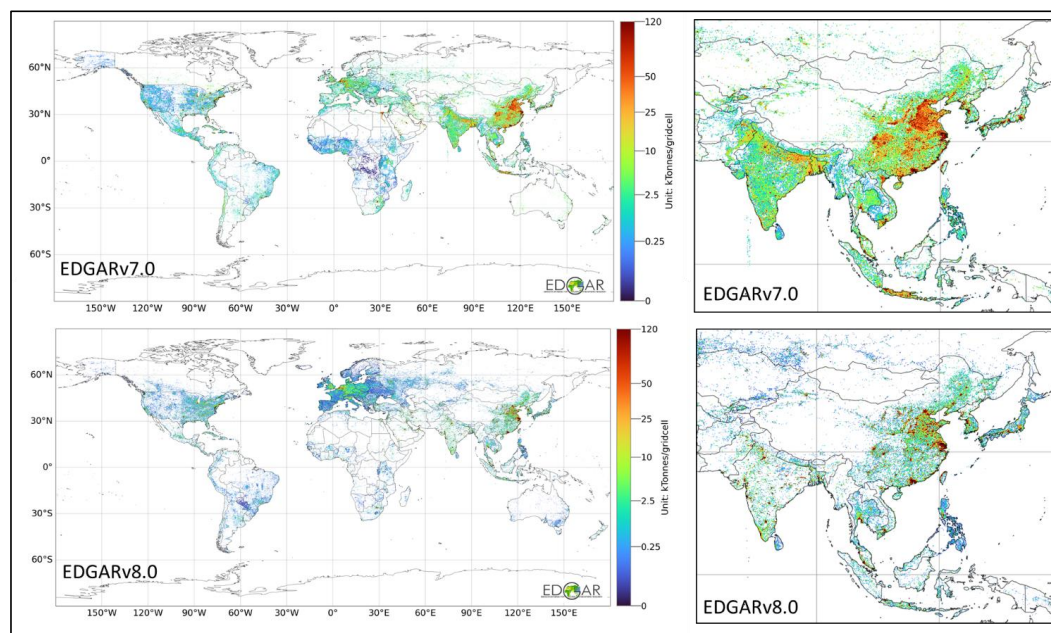
297 **Figure 5 – N<sub>2</sub>O emissions from manure management at global level and in Europe, where intensive livestock**  
298 **activities appear as emission hot-spots.**

### 299 **3.5 Gap-filling missing information of point sources**

300 A significant improvement is represented by the development and use of a new spatial proxy  
301 to gap-fill missing information for all industrial related emissions. Until EDGARv7.0,  
302 population related proxies were used as backup information when no spatial data was available  
303 to represent the emissions for a sector within a country (Crippa et al., 2021). However, here we  
304 decided to use the non-residential built-up surface information developed by the Global Human  
305 Settlements Layer (GHSL) (Pesaresi and Politis, 2023; European Commission, 2023) as  
306 backup proxy to distribute the emissions of all the activities not related with small-scale  
307 combustion for which no point source information was available (even for individual  
308 countries). For certain sectors and regions, this non-residential gap-filling proxy is also used to



309 allocate a fraction of the emissions of a certain sector (refer for example to the industrial  
 310 facilities section for Europe). The overall effect of using this new proxy is a change in the  
 311 industrial contribution over densely populated areas which was previously higher in EDGAR  
 312 compared to other inventories in particular over Europe (Thunis et al., 2023). Figure 6 shows  
 313 CO<sub>2</sub> emission maps from manufacturing industries obtained in EDGARv7.0 and EDGARv8.0.  
 314 This comparison figure highlights the implications of using different gap-filling proxies for the  
 315 industrial sector, and in particular those based on population (EDGARv7.0) and the new ones  
 316 based on non-residential built-up surface data used in EDGARv8.0. Overall, using non-  
 317 residential built-up information to allocate emissions of industrial activities to complement  
 318 point source information leads to lower emission levels allocated to urban areas and a less  
 319 densely distributed map over certain regions (e.g. China, India, etc.). Figure S3 shows the  
 320 impact of this update on global fossil CO<sub>2</sub> emissions from the industrial sector over global  
 321 Functional Urban Areas (FUAs) in 2022. The ratio between these emissions over FUAs is  
 322 typically higher, on average by around 30%, in EDGARv8.0 than in EDGARv7.0 for several  
 323 developing countries (e.g. Africa, South America, India, etc.) due to the presence of industrial  
 324 point sources and non-residential activities still close to urban areas. On the opposite, lower  
 325 (on average around 20% less) emissions from industries are found in many industrialised  
 326 regions (e.g. Europe, USA, Oceania) due to the displacement of industrial activities in remote  
 327 areas or outside the FUAs. This result represents the effect of using non-population based  
 328 proxies for industrial emissions in EDGARv8.0 compared to previous EDGAR proxies.



329  
 330 **Figure 6 – CO<sub>2</sub> emissions from industrial combustion in 2021 from EDGARv7.0 and v8.0, showing the**  
 331 **impact of the gap-filling proxies used for industrial sources.**

332 **4 Linear sources of emissions: international shipping**

333 Since EDGARv6.0, international shipping emissions are distributed using the STEAM (Ship  
 334 Traffic Emission Assessment Model) model from the Finnish Meteorological Institute

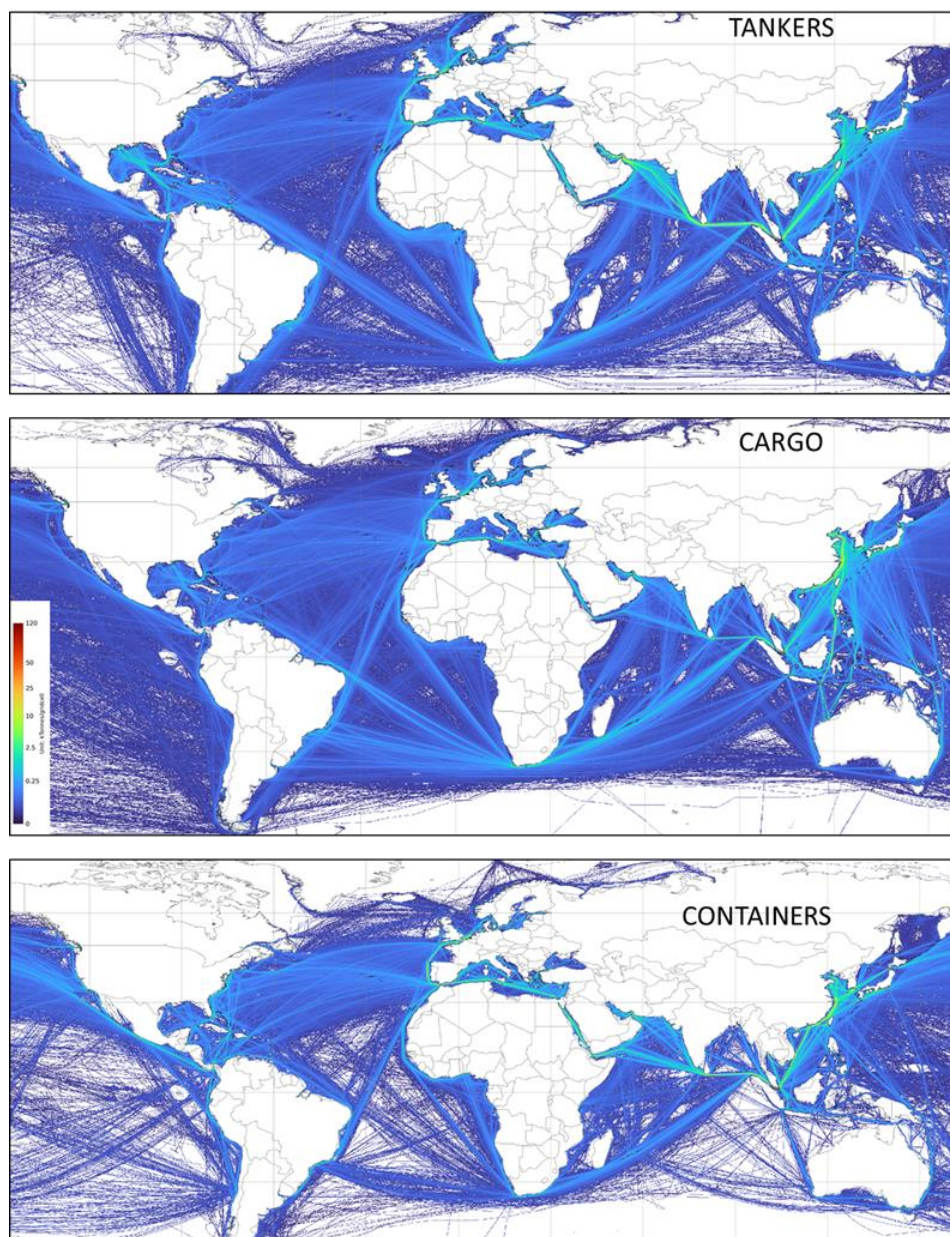


335 (Jalkanen et al., 2012; Johansson et al., 2017). Emissions are distributed on yearly basis from  
336 2000 till 2018, including multi vessels information (cargo, container, fishing, passenger  
337 cruisers, service, tankers, vehicle carriers, miscellaneous). Compared to the previous EDGAR  
338 proxy, the use of the STEAM data allows a better representation of the evolution in time of the  
339 international shipping emissions, differentiating on yearly basis the variation of the routes and  
340 their intensity for the different vessels consistently with the information available in EDGAR  
341 (see Fig. 7). Only data covering sea areas are included, since inland data over big rivers or lakes  
342 is not robust yet to be included in EDGAR. Information on Emission Control Areas (ECAs),  
343 and in particular on sulphur emission control areas (SECAs) and NO<sub>x</sub> emission control areas  
344 (NECAs), are not yet included, while it represents one of the future updates of EDGAR. A  
345 comparison between international shipping intensities as available in EDGAR before and after  
346 this update is presented in Fig. S4 of the Supplement.

347 Figure 8 focusses on three main vessel types representing the largest fraction of GHG emissions  
348 from international shipping in 2022 and contributing specifically for around 22% (tankers),  
349 24% (containers) and 28% (cargo) to total international shipping GHG emissions. The impact  
350 of using the STEAM data to develop the new spatial proxies for international shipping is shown  
351 in Fig. 8, where the comparison between EDGARv5 and EDGARv8 CO<sub>2</sub> emissions from the  
352 three main vessel types over the different Oceans and Seas is presented. EDGARv5 proxies  
353 were allocating most of the international shipping emissions over the Atlantic and Pacific  
354 Oceans, while the new proxies of EDGARv8 allocate the largest portion of these emissions  
355 (40%) over the Seas around China, Japan and Philippines. The relative share of tankers  
356 emissions over the Mediterranean Sea is also very different between the two versions, with the  
357 largest contribution (85%) among the three considered categories in EDGARv5. Two times  
358 higher emissions are also allocated to the Gulf of Mexico and Arabian Sea when using the  
359 STEAM based proxies in EDGARv8.

360

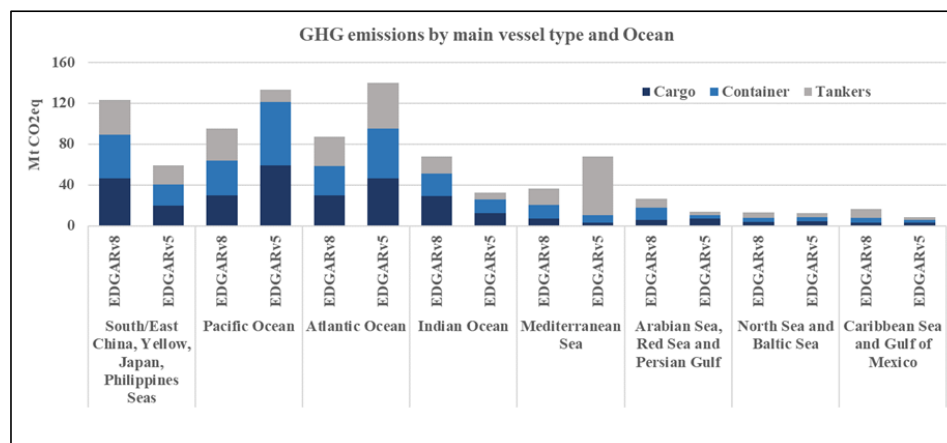
361



362

363 **Figure 7 – International shipping GHG emissions (2021) with the ship tracks for tankers, containers and**  
364 **cargo vessels as in EDGARv8.0.**

365



366

367 **Figure 8 – Comparison of GHG emissions from international shipping (2022) by main vessel type and**  
368 **Ocean from EDGARv5 and EDGARv8. Fishing, services and passenger related emissions are excluded**  
369 **from this comparison.**

## 370 **5 Area sources of emissions**

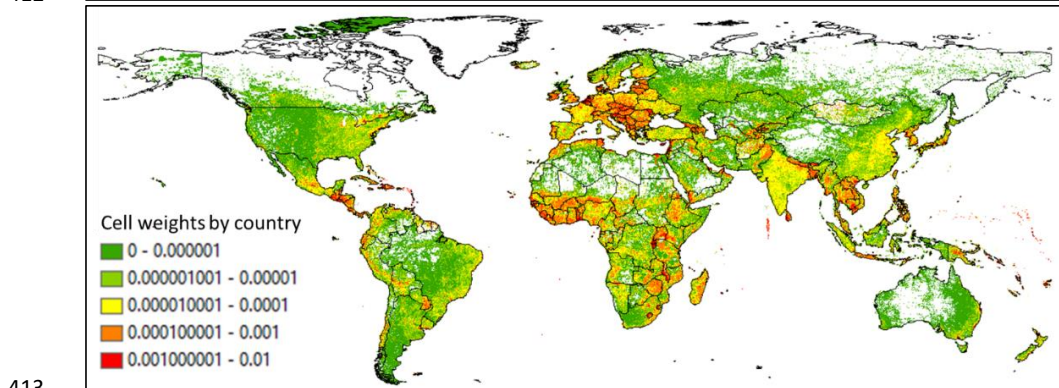
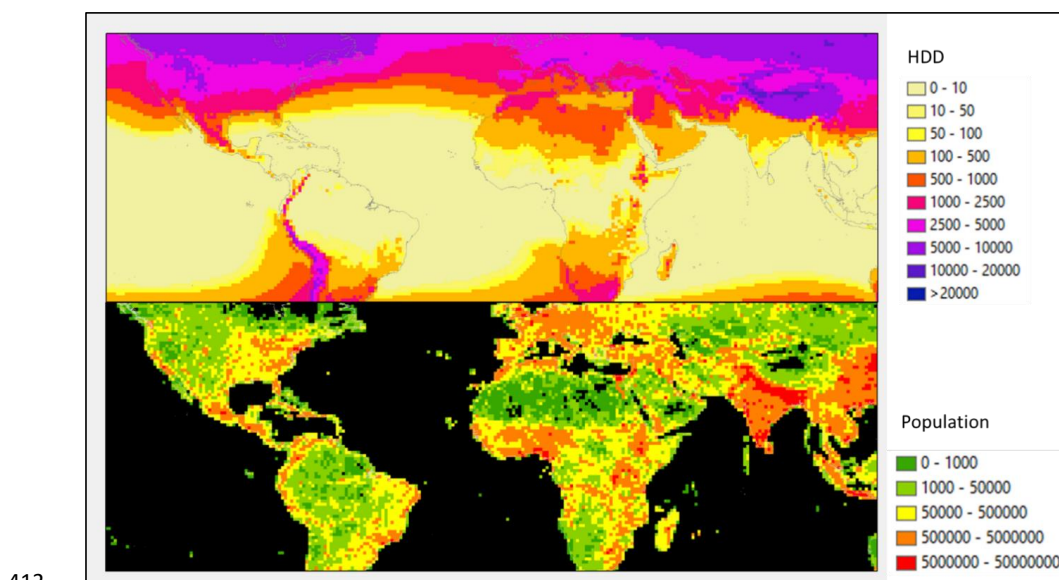
### 371 **5.1 Residential activities**

372 Small-scale combustion emissions are mostly related with non-industrial activities, such as  
373 those from the residential, commercial and agricultural/fishing sectors. Therefore, population  
374 based spatial proxies are often used to downscale national emissions. EDGARv8.0 aims at  
375 coupling population distribution with heating degree days since the amount of emissions is not  
376 only dependent on the number of people living over certain areas, but also on the  
377 meteorological conditions and the heating needs for indoor spaces. Residential emissions are  
378 therefore distributed considering both population intensities and heating needs, with varying  
379 profiles from 1970 to 2022. EDGARv8.0 includes the latest population gridmaps developed by  
380 the Global Human Settlements GHS-POP R2023A (Schiavina et al., 2023b; Freire et al., 2016),  
381 which comprise residential population information for 12 epochs, starting from 1975 to 2020  
382 with 5-years time steps and projections to 2025 and 2030 obtained distributing over global  
383 gridmaps census data from CIESIN GPWv4.11. GHS-POP R2023A data at 30 arc-seconds  
384 (WGS84, EPSG:4326) (or about 1km) spatial resolution were used to develop the corresponding  
385 spatial proxies in EDGAR. Population density is then calculated for each gridcell and it is used  
386 as a proxy to allocate household emissions over populated areas. Small-scale combustion  
387 activities related with agriculture are distributed using rural population maps obtained from the  
388 GHS-SMOD R2023 product (including only low and very low density rural grid cells)  
389 (Schiavina et al., 2023a). For missing years, the closest population map to each epoch is taken  
390 (e.g. for the years 2001 and 2002 the population map is the one of 2000, while for the years  
391 2003 and 2004 it is the one of 2005).

392 To account for the effect of the weather (ambient temperature) on heating needs in the  
393 residential sector, heating degree days (HDD) have been computed using the 2 meters  
394 temperature data with hourly time resolution and 1 degree spatial resolution using the  
395 Copernicus ERA5 atmospheric reanalysis produced by ECMWF for the years 1970-2022  
396 (<https://cds.climate.copernicus.eu/cdsapp#!/dataset/reanalysis-era5-single-levels?tab=form>).



397 HDD is the cumulative number of degrees by which the mean daily temperature falls below a  
398 reference temperature (usually 18 °C or 19 °C which is adequate for human comfort). HDD  
399 were calculated following the methodology described by Spinoni et al. (2018) and assuming a  
400 reference temperature of 18°C. Cooling Degree Days (CDD) are not included in the  
401 development of the spatial proxies since they are mainly related with electricity consumption  
402 rather than to fuel combustion in the residential sector. An additional weight to the population  
403 distribution is therefore added by the HDD metric, thus increasing the emissions arising in  
404 colder regions subjected to more heating needs rather than in warm areas for the same amount  
405 of population. Our approach does not aim at identifying and representing the heating habits for  
406 all countries, while modulating within a single country the combustion of fuels for e.g. heating  
407 purposes due to the different temperatures across latitudes (climatic zones). Countries may  
408 have in fact different habits in turning on and off their heating systems, thus requiring the use  
409 of different reference temperature values in the calculation of HDD (Atalla et al., 2018) which  
410 is not taken into account here. The process to build the residential proxy in EDGAR is shown  
411 in Fig. 9.





414 **Figure 9 – Coupling heating degree days (a) and population density (b) as a proxy (c) to downscale**  
415 **residential emissions. Data refer to the year 2020.**

416

## 417 **6 Results**

418 The purpose of this work is to describe the methodological improvements included in  
419 EDGARv8.0 linked to the update of the spatial data used to downscale country and sector  
420 specific emissions. In addition, a specific focus is dedicated to case studies showing the  
421 relevance of understanding the evolution of GHG emissions at sub-national level in order to  
422 support the development of regional climate mitigation and adaptation policies (Kuramochi et  
423 al., 2020). Therefore, the reader can refer to Crippa et al. (2023c) for the description of country  
424 and sector specific GHG emission trends at global level. In the following sections, insights on  
425 the global distribution of GHG emissions as well as their sub-national features are described.

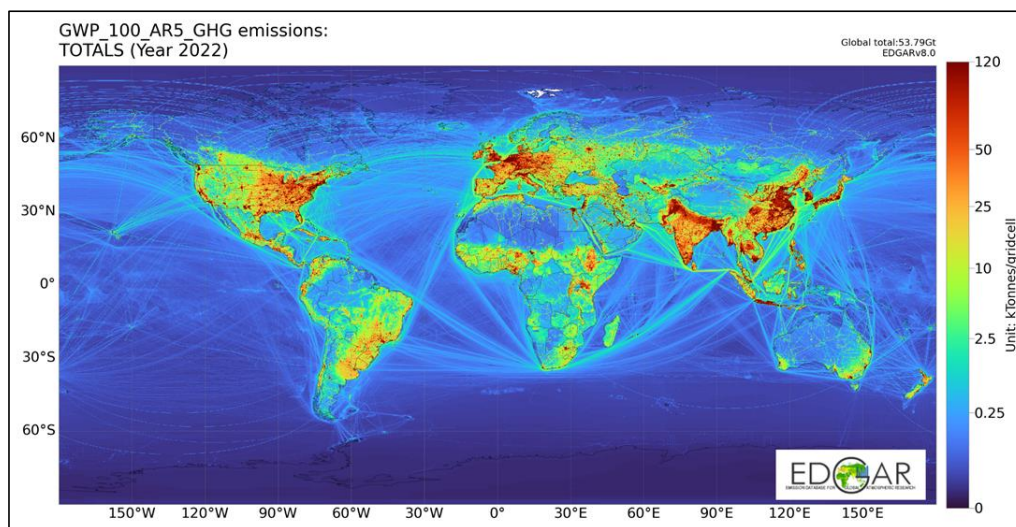
### 426 **6.1 Global GHG emissions in EDGARv8.0**

427 Figure 10 shows global GHG emissions in 2022 as a result of the EDGARv8 gridding process,  
428 while Figure 11 reports the same emissions at country and sub-national level. Complementary  
429 figures are also reported in the Supplement (Figs. S5-S8) showing the evolution of GHG, fossil  
430 CO<sub>2</sub>, CH<sub>4</sub> and N<sub>2</sub>O global emission maps from 1970 to 2022.

431 The main strength and novelty of EDGARv8.0 is related with the production of a global GHG  
432 emission database at different level of granularity in support of local, regional and global  
433 climate actions. The high spatial resolution global maps are available at 0.1°x0.1° WGS84  
434 (EPSG4326), about 10km at the equator, both as emissions and emission fluxes (.txt and .NetCDF  
435 files, [https://edgar.jrc.ec.europa.eu/dataset\\_ghg80](https://edgar.jrc.ec.europa.eu/dataset_ghg80)) fulfilling the requirements of the global  
436 atmospheric modelling community but also bridging bottom-up and top-down (mostly satellite  
437 based) GHG emission estimates (see Fig. 10).

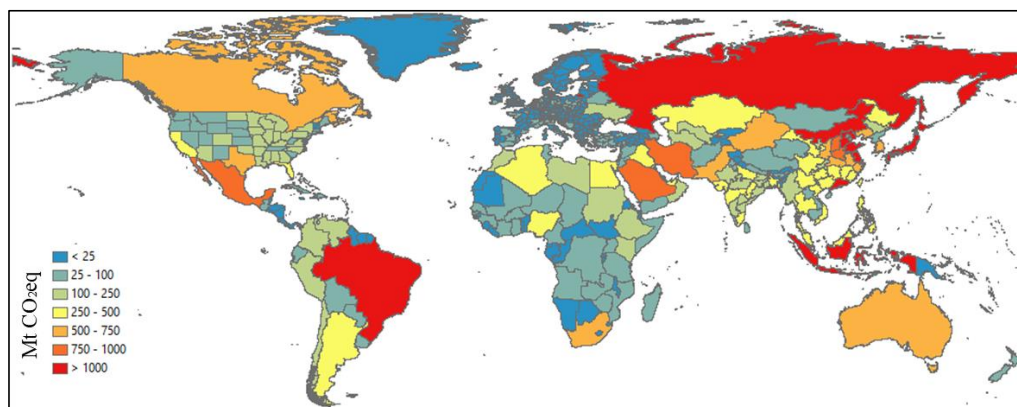
438 EDGARv8.0 allows full flexibility in the aggregation of emissions at sub-national level, thus  
439 supporting the analysis of the spatio-temporal variability of the emissions not only at gridcell  
440 level but also over wider administrative domains, or areas of interest such as urban centres  
441 (Melchiorri, 2022). A second key product from EDGARv8.0 is represented by GHG emissions  
442 at sub-national level using the Global ADMinistrative layer version 4.1 at level 1 and NUTS2  
443 level for the EU extended geographical domain, as shown in Fig. 11. In the next sections, case  
444 studies over the European, American and Asian domains are discussed more in detail.





445

446 **Figure 10 – Global GHG emission map in 2022 from EDGARv8.0.**



447

448 **Figure 11 – Global GHG emissions by country and sub-national level in 2022 based on EDGARv8.0.**

449

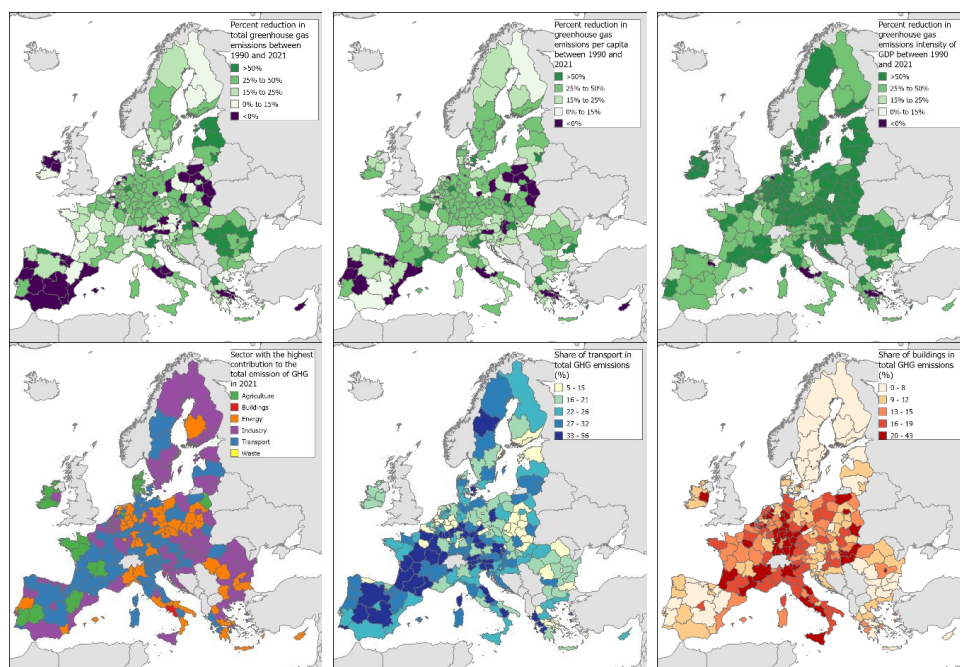
## 450 **6.2 Sub-national emissions: the EU case**

451 Climate and environmental territorial policies require robust and consistent knowledge of  
452 greenhouse gas (GHG) and air pollutant emissions at sub-national level (e.g. NUTS2). No sub-  
453 national official reporting is available and the high spatial resolution data of EDGAR fill this  
454 knowledge gap. EDGAR sub-national GHG emissions are used as reference by the European  
455 Commission in Cohesion Reports (European Commission, 2022), the EU semester process or  
456 Climate Action territorial analysis. Figure 12 shows how GHG emissions at NUTS2 level have  
457 changed from 1990 to 2021 both in absolute, per capita and per GDP terms. Out of 242 EU  
458 regions, 155 regions shown a downward trend since 1990, while 206 and 204 since 2005 (on  
459 average -1.27% per year) and 2010 (on average -1.35% per year), respectively. However, in  
460 2021, only 34 regions reached less than 5t CO<sub>2</sub>eq/person which corresponds to the average



461 value needed to achieve the 2030 EU climate targets. The most contributing sectors to total EU  
 462 GHG emissions in 2021 are the power generation (27%), industry (23%), transportation (20%),  
 463 buildings (14%) and agriculture (11%), showing the different regions in the EU have different  
 464 transition challenges. For example, when looking at NUTS2 level (see Fig. 12, middle bottom  
 465 panel) the transport sector often represents the sector with the largest contribution at regional  
 466 level, in particular in rural regions of Spain, France, Italy, or Germany. Figure 12 (bottom right  
 467 panel) also shows the share of GHG emissions arising from small-scale combustion (buildings  
 468 sector) at NUTS2 level, highlighting several regions for which this sector contributes more  
 469 than 15-20% to the regional total.

470



471

472 **Figure 12 – Relative change of European GHG emissions by NUTS2 between 1990 and 2021 (top panels).**  
 473 **Sector contribution of European GHG emissions by NUTS2 in 2021 (bottom panels). The sector with the**  
 474 **highest contribution in 2021 for each NUTS2 is shown in the map on the left panel. The share of GHG**  
 475 **emissions from transport (middle panel) and buildings (right panel) to total emissions in Europe by**  
 476 **NUTS2 is also shown.**

477

478

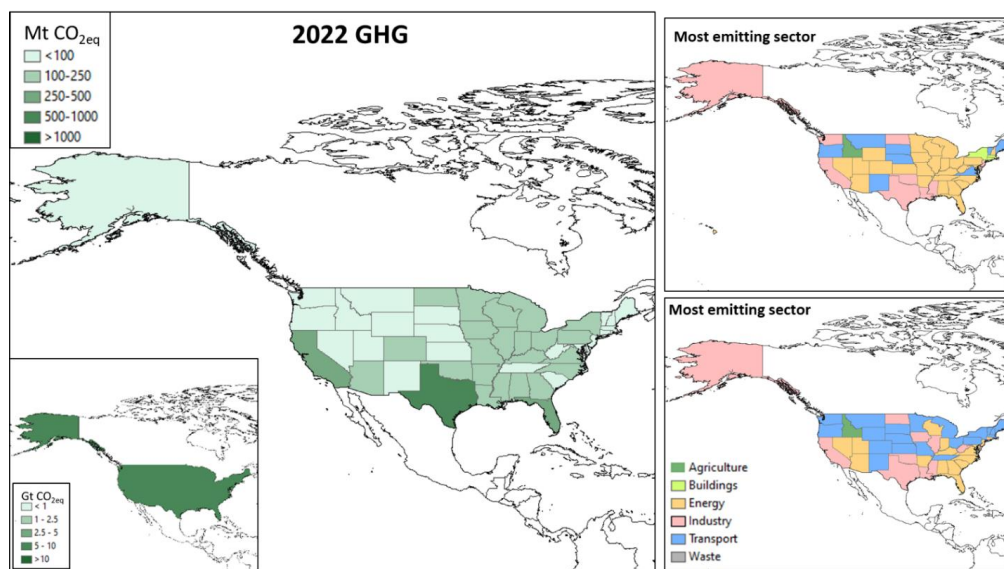
### 479 6.3 Sub-national emissions in the United States, China and India

480 EDGARv8.0 includes GHG emission estimates at sub-national level also for the United States  
 481 (i.e. estimates for each US state, Fig. 13), for each Chinese province and each Indian state (Fig.  
 482 14). Based on our analysis, Texas emits 11.5% of the total US GHG emissions in 2022,  
 483 followed by California with a contribution of 7.7% and Florida with a share of 4.6%. Also in



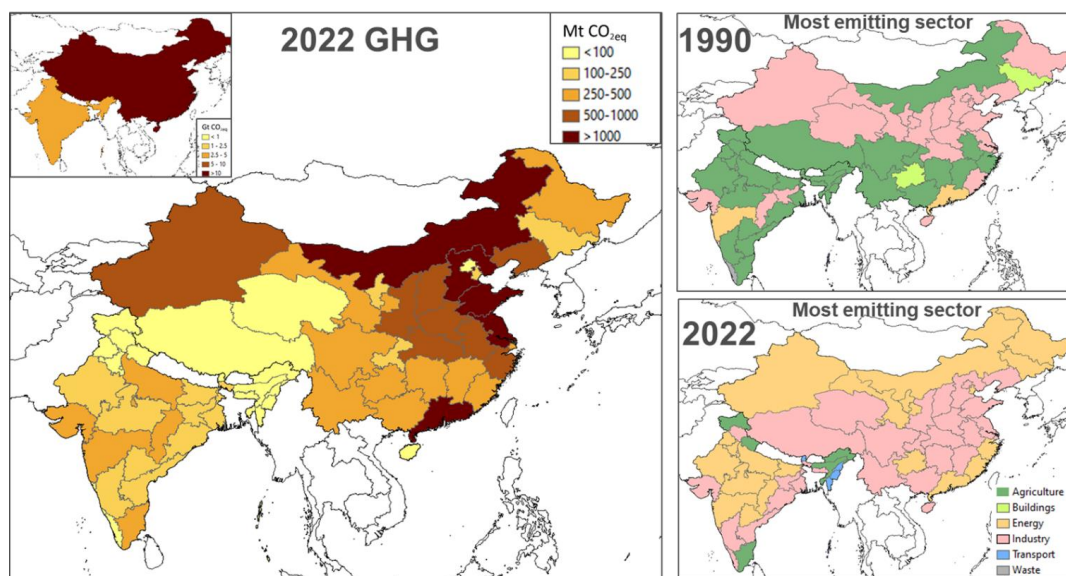
484 1990, Texas and California were the most emitting states, followed by Ohio, Pennsylvania and  
485 Illinois. Over the past 3 decades, the sector with the highest share of GHGs at state level over  
486 the US has changed, with a shift from power and industry towards transport (see Fig. 13).

487 In 2022, 5 most emitting Chinese provinces contributed for around 40% of the Chinese total  
488 GHG emissions and they were Shandong (8.9% of the country total), Guangdong (8.4%),  
489 Jiangsu (7.4%), Hebei (6.6%) and Nei Mongol (6.5%), consistently with some literature studies  
490 addressing province level CO<sub>2</sub> and GHG emissions in China (Jiang et al., 2019; Zhang et al.,  
491 2020). In 1990, the top 5 emitting provinces were Shandong (8.1%), Hebei (6.5%), Jiangsu  
492 (6.2%), Henan (5.9%) and Nei Mongol (5.8%) contributing for around 30% to the Chinese  
493 total GHG emissions. In 2022, 5 Indian states emitted around 50% of the country total GHG  
494 emissions, namely Maharashtra (11.8%), Tamil Nadu (11.7%), Uttar Pradesh (8.1%), Gujarat  
495 (8.0%), Chhattisgarh (6.6%). In 1990, the most emitting Indian states were Tamil Nadu  
496 (18.4%), Maharashtra (9.5%), Uttar Pradesh (9.3%), West Bengal (6.6%), Andhra Pradesh  
497 (6.0%). Compared to the US and Europe cases, a different picture is found over the Asian  
498 domain in terms of most emitting sectors at sub-national level (Fig. 14). The effect of the  
499 economic growth and the transition from an agricultural based towards a more industrialised  
500 economy can be seen in Fig. 14 (right panels). As a result, the sectors with the highest share  
501 changed from agriculture (in 1990) to energy and industry (in 2022) over China and India,  
502 with the exception of few regions (e.g. Tamil Nadu, Assam, Jammu and Kashmir, Uttarakhand)  
503 which kept an agriculture based economy also in 2022. This type of information and analysis  
504 is instrumental for the definition of effective sector specific climate mitigation actions at sub-  
505 national level.



506

507 **Figure 13 - 2022 GHG emissions at sub-national level in the United States are represented left panel and**  
508 **the sector with the highest contribution in 1990 and 2022 for each US state is shown in the maps on the**  
509 **right.**



510

511 **Figure 14 - 2022 GHG emissions at sub-national level over the Asian domain, with focus on China and**  
512 **India, (left panel) and the sector with the highest contribution in 1990 and 2022 for each Chinese and Indian**  
513 **province/state is shown in the maps on the right.**

## 514 7 Data availability

515 The EDGARv8.0 GHG global emission maps can be freely accessed at  
516 <https://doi.org/10.2905/b54d8149-2864-4fb9-96b9-5fd3a020c224> (Crippa, 2023a). The  
517 EDGARv8.0 subnational emissions can be accessed at [doi:10.2905/D67EEDA8-C03E-4421-](https://doi.org/10.2905/D67EEDA8-C03E-4421-95D0-0ADC460B9658)  
518 [95D0-0ADC460B9658](https://doi.org/10.2905/D67EEDA8-C03E-4421-95D0-0ADC460B9658) (Crippa et al., 2023b). All data can also be accessed through the  
519 EDGAR website at [https://edgar.jrc.ec.europa.eu/dataset\\_ghg80](https://edgar.jrc.ec.europa.eu/dataset_ghg80) and  
520 [https://edgar.jrc.ec.europa.eu/dataset\\_ghg80\\_nuts2](https://edgar.jrc.ec.europa.eu/dataset_ghg80_nuts2) (last access: November 2023).

521 Data are made available as emission gridmaps for each substance and for total GHGs as .txt  
522 and .nc files with emissions expressed in ton substance/0.1degree x 0.1degree/year. Emission  
523 fluxes are available as .nc files and they are expressed in kg substance/m<sup>2</sup>/s. Emission maps  
524 are available both as total and sector specific emissions.

## 525 8 Conclusions

526 Climate targets are often set at global and national level but the implementation of mitigation  
527 actions occurs at local and regional level. It is therefore of utmost relevance developing sub-  
528 national GHG emission for policy development and to monitor the progress towards climate  
529 targets or to evaluate their impacts. This work summarises the main updates developed within  
530 the Emissions Database for Global Atmospheric Research (EDGAR) for what concerns the use  
531 of high resolution and up to date spatial information to improve the global geospatial  
532 disaggregation of GHG emissions at sub-national level. Having accurate and up to date sector  
533 specific GHG emission global maps at high spatial resolution (0.1x0.1 degrees) is instrumental  
534 for the design of effective climate mitigation options beyond national climate targets.  
535 EDGARv8.0 spatial proxies include globally consistent spatial data derived for example from  
536 the Global Energy Monitor, the Global Human Settlements Layer work, satellite based



537 information to compute heating degree days or to identify hot-spots from agricultural activities,  
538 the STEAM model for ship track and many other global datasets. The use of satellite data to  
539 improve the EDGAR spatial proxies represents a successful cooperation between bottom-up  
540 inventory compilers and the Earth observation community, and the possibility to integrate  
541 relevant satellite based datasets and statistical information. In addition, EDGARv8.0 integrates  
542 spatial information from local databases (e.g. EPRTR for Europe, EIA data for the US) when  
543 including more detailed data compared to what available in global databases. A further  
544 improvement within EDGAR is related with the inclusion of sub-national information,  
545 representing a unique feature to address in a consistent way the evaluation of spatial patterns  
546 in the evolution of sub-national GHG emissions. Such spatial resolution and sub-national sector  
547 specific variability sets the ground for the production of city level emission data records, as  
548 used for example in the Urban Centre Database  
549 ([https://ghsl.jrc.ec.europa.eu/ghs\\_stat\\_ucdb2015mt\\_r2019a.php](https://ghsl.jrc.ec.europa.eu/ghs_stat_ucdb2015mt_r2019a.php)). In this paper, few case  
550 studies are presented, with main focus on the European case where the EDGAR sub-national  
551 data are regularly used as input for the EU Semesters and contribute to climate action territorial  
552 and cohesion policies through the EU Cohesion Reports.

553

## 554 **9 Acknowledgements**

555 We are grateful to the EDGAR team (M. Crippa, D. Guizzardi, E. Schaaf, M. Muntean, F.  
556 Pagani, M. Banja, W. Becker and F. Monforti-Ferrario) for the work needed to publish the  
557 EDGARv8.0 greenhouse gas emission datasets ([https://edgar.jrc.ec.europa.eu/dataset\\_ghg80](https://edgar.jrc.ec.europa.eu/dataset_ghg80)).  
558 The views expressed in this publication are those of the author(s) and do not necessarily reflect  
559 the views or policies of the European Commission. All emissions, except for CO<sub>2</sub> emissions  
560 from fuel combustion, are from the EDGAR (Emissions Database for Global Atmospheric  
561 Research) Community GHG database comprising IEA-EDGAR CO<sub>2</sub>, EDGAR CH<sub>4</sub>, EDGAR  
562 N<sub>2</sub>O and EDGAR F-gases version 8.0 (2023). IASI-NH<sub>3</sub> catalogue was updated in the  
563 framework of the ESA World Emission project (<https://www.world-emission.com/>). [The ULB](#)  
564 [also gratefully acknowledges support from the TAPIR project \(Air Liquide Foundation\)](#).

## 565 **10 References**

566 Atalla, T., Gualdi, S., and Lanza, A.: A global degree days database for energy-related  
567 applications, *Energy*, 143, 1048-1055, <https://doi.org/10.1016/j.energy.2017.10.134>, 2018.

568 CEIP: Inventory Review 2021 Review of emission data reported under the LRTAP  
569 Convention,  
570 [https://www.ceip.at/fileadmin/inhalte/ceip/00\\_pdf\\_other/2021/inventoryreport\\_2021.pdf](https://www.ceip.at/fileadmin/inhalte/ceip/00_pdf_other/2021/inventoryreport_2021.pdf), Last  
571 Access: August 2023., 2021.

572 Clarisse, L., Van Damme, M., Clerbaux, C., and Coheur, P. F.: Tracking down global NH<sub>3</sub>  
573 point sources with wind-adjusted superresolution, *Atmos. Meas. Tech.*, 12, 5457-5473,  
574 10.5194/amt-12-5457-2019, 2019.

575 Crippa, M., Guizzardi, D., Pagani, F., and Pisoni, E.: GHG Emissions at sub-national level,  
576 European Commission, Joint Research Centre (JRC) [Dataset] doi:10.2905/D67EEDA8-  
577 C03E-4421-95D0-0ADC460B9658 PID: [http://data.europa.eu/89h/d67eeda8-c03e-4421-  
578 95d0-0adc460b9658](http://data.europa.eu/89h/d67eeda8-c03e-4421-95d0-0adc460b9658), 2023b.



- 579 Crippa, M., Guizzardi, D., Pisoni, E., Solazzo, E., Guion, A., Muntean, M., Florczyk, A.,  
580 Schiavina, M., Melchiorri, M., and Hutfilter, A. F.: Global anthropogenic emissions in urban  
581 areas: patterns, trends, and challenges, *Environmental Research Letters*, 16, 074033,  
582 10.1088/1748-9326/ac00e2, 2021.
- 583 Crippa, M., Guizzardi, D., Muntean, M., Schaaf, E., Dentener, F., van Aardenne, J. A., Monni,  
584 S., Doering, U., Olivier, J. G. J., Pagliari, V., and Janssens-Maenhout, G.: Gridded emissions  
585 of air pollutants for the period 1970–2012 within EDGAR v4.3.2, *Earth Syst. Sci. Data*, 10,  
586 1987-2013, 10.5194/essd-10-1987-2018, 2018.
- 587 Crippa, M., Guizzardi, D., Pagani, F., Banja, M., Muntean, M., Schaaf, E., Becker, W.,  
588 Monforti-Ferrario, F., Quadrelli, R., Riskey Martin, A., Taghavi-Moharamli, P., Köykkä, J.,  
589 Grassi, G., Rossi, S., Brandao De Melo, J., Oom, D., Branco, A., San-Miguel, J., and Vignati,  
590 E.: GHG emissions of all world countries, Publications Office of the European Union,  
591 Luxembourg, doi:10.2760/953322, JRC134504, 2023c.
- 592 Crippa, M., Guizzardi, D., Pagani, F., Banja, M., Muntean, M., Schaaf, E., Becker, W., Monforti-  
593 Ferrario, F., Quadrelli, R., Riskey Martin, A., Taghavi-Moharamli, P., Grassi, G., Rossi, S.,  
594 Brandao De Melo, J., Oom, D., Branco, A., San-Miguel, J., Vignati, E.: EDGAR v8.0  
595 Greenhouse Gas Emissions, European Commission, Joint Research Centre (JRC) [Dataset] doi:  
596 10.2905/b54d8149-2864-4fb9-96b9-5fd3a020c224 PID: [http://data.europa.eu/89h/b54d8149-  
597 2864-4fb9-96b9-5fd3a020c224](http://data.europa.eu/89h/b54d8149-2864-4fb9-96b9-5fd3a020c224), 2023a.
- 598 Elvidge, C. D., Baugh, K., Zhizhin, M., Hsu, F. C., and Ghosh, T.: Supporting international  
599 efforts for detecting illegal fishing and GAS flaring using viirs, 2017 IEEE International  
600 Geoscience and Remote Sensing Symposium (IGARSS), 23-28 July 2017, 2802-2805,  
601 10.1109/IGARSS.2017.8127580,
- 602 EPTR: E-PRTR database v18, [https://www.eea.europa.eu/data-and-maps/data/member-  
603 states-reporting-art-7-under-the-european-pollutant-release-and-transfer-register-e-prtr-  
604 regulation-23/european-pollutant-release-and-transfer-register-e-prtr-data-  
605 base/eptr\\_v9\\_csv.zip](https://www.eea.europa.eu/data-and-maps/data/member-states-reporting-art-7-under-the-european-pollutant-release-and-transfer-register-e-prtr-regulation-23/european-pollutant-release-and-transfer-register-e-prtr-data-base/eptr_v9_csv.zip), 2020.
- 606 European Commission: Cohesion in Europe towards 2050 - Eighth report on economic, social  
607 and territorial cohesion, doi: 10.2776/624081, 2022.
- 608 European Commission: GHSL Data Package 2023, Publications Office of the European Union,  
609 Luxembourg, JRC133256, doi:10.2760/098587, 2023.
- 610 European Union: European Commission, Joint Research Centre (JRC), EDGAR (Emissions  
611 Database for Global Atmospheric Research) Community GHG database, comprising IEA-  
612 EDGAR CO<sub>2</sub>, EDGAR CH<sub>4</sub>, EDGAR N<sub>2</sub>O and EDGAR F-gases version 8.0 (2023). Unless  
613 otherwise noted, all material owned by the European Union is licensed under the Creative  
614 Commons Attribution 4.0 International (CC BY 4.0) licence. This means that reuse is allowed,  
615 provided that appropriate credit is given and any changes are indicated, 2023.
- 616 EUROSTAT: [https://ec.europa.eu/eurostat/web/gisco/geodata/reference-data/administrative-  
617 units-statistical-units/nuts](https://ec.europa.eu/eurostat/web/gisco/geodata/reference-data/administrative-units-statistical-units/nuts), 2021.



- 618 Feng, L., Smith, S. J., Braun, C., Crippa, M., Gidden, M. J., Hoesly, R., Klimont, Z., van Marle,  
619 M., van den Berg, M., and van der Werf, G. R.: The generation of gridded emissions data for  
620 CMIP6, *Geosci. Model Dev.*, 13, 461-482, 10.5194/gmd-13-461-2020, 2020.
- 621 Freire, S., MacManus, K., Pesaresi, M., Doxsey-Whitfield, E., and Mills, J.: Development  
622 of new open and free multi-temporal global population grids at 250 m resolution, *Geospatial*  
623 *Data in a Changing World*, Association of Geographic Information Laboratories in Europe  
624 (AGILE), 2016.
- 625 Global Energy Monitor: Global Gas Plant Tracker,  
626 <https://globalenergymonitor.org/projects/global-gas-plant-tracker/>, 2022a.
- 627 Global Energy Monitor: Global Coal Mine Tracker,  
628 <https://globalenergymonitor.org/projects/global-coal-mine-tracker/>, 2022b.
- 629 Global Energy Monitor: Global steel plant tracker,  
630 <https://globalenergymonitor.org/projects/global-steel-plant-tracker/>, 2022c.
- 631 Global Energy Monitor: Global Coal Plant Tracker,  
632 <https://globalenergymonitor.org/projects/global-coal-plant-tracker/>, 2022d.
- 633 Guevara, M., Enciso, S., Tena, C., Jorba, O., Dellaert, S., Denier van der Gon, H., and Pérez  
634 García-Pando, C.: A global catalogue of CO<sub>2</sub> emissions and co-emitted species from power  
635 plants at a very high spatial and temporal resolution, *Earth Syst. Sci. Data Discuss.*, 2023, 1-  
636 41, 10.5194/essd-2023-95, 2023.
- 637 Hoesly, R. M., Smith, S. J., Feng, L., Klimont, Z., Janssens-Maenhout, G., Pitkanen, T.,  
638 Seibert, J. J., Vu, L., Andres, R. J., Bolt, R. M., Bond, T. C., Dawidowski, L., Kholod, N.,  
639 Kurokawa, J. I., Li, M., Liu, L., Lu, Z., Moura, M. C. P., O'Rourke, P. R., and Zhang, Q.:  
640 Historical (1750–2014) anthropogenic emissions of reactive gases and aerosols from the  
641 Community Emissions Data System (CEDS), *Geosci. Model Dev.*, 11, 369-408, 10.5194/gmd-  
642 11-369-2018, 2018.
- 643 IEA-EDGAR CO<sub>2</sub>: A component of the EDGAR (Emissions Database for Global Atmospheric  
644 Research) Community GHG database version 8.0 (2023) including or based on data from IEA  
645 (2022) Greenhouse Gas Emissions from Energy, [www.iea.org/data-and-statistics](http://www.iea.org/data-and-statistics), as modified  
646 by the Joint Research Centre, 2023.
- 647 Jalkanen, J. P., Johansson, L., Kukkonen, J., Brink, A., Kalli, J., and Stipa, T.: Extension of an  
648 assessment model of ship traffic exhaust emissions for particulate matter and carbon monoxide,  
649 *Atmos. Chem. Phys.*, 12, 2641-2659, 10.5194/acp-12-2641-2012, 2012.
- 650 Janssens-Maenhout, G., Crippa, M., Guizzardi, D., Muntean, M., Schaaf, E., Dentener, F.,  
651 Bergamaschi, P., Pagliari, V., Olivier, J. G. J., Peters, J. A. H. W., van Aardenne, J. A., Monni,  
652 S., Doering, U., Petrescu, A. M. R., Solazzo, E., and Oreggioni, G. D.: EDGAR v4.3.2 Global  
653 Atlas of the three major greenhouse gas emissions for the period 1970–2012, *Earth Syst. Sci.*  
654 *Data*, 11, 959-1002, 10.5194/essd-11-959-2019, 2019.
- 655 Jiang, J., Ye, B., and Liu, J.: Peak of CO<sub>2</sub> emissions in various sectors and provinces of China:  
656 Recent progress and avenues for further research, *Renewable and Sustainable Energy Reviews*,  
657 112, 813-833, <https://doi.org/10.1016/j.rser.2019.06.024>, 2019.



- 658 Johansson, L., Jalkanen, J.-P., and Kukkonen, J.: Global assessment of shipping emissions in  
659 2015 on a high spatial and temporal resolution, *Atmospheric Environment*, 167, 403-415,  
660 <https://doi.org/10.1016/j.atmosenv.2017.08.042>, 2017.
- 661 Kuenen, J., Dellaert, S., Visschedijk, A., Jalkanen, J. P., Super, I., and Denier van der Gon, H.:  
662 CAMS-REG-v4: a state-of-the-art high-resolution European emission inventory for air quality  
663 modelling, *Earth Syst. Sci. Data*, 14, 491-515, 10.5194/essd-14-491-2022, 2022.
- 664 Kuramochi, T., Roelfsema, M., Hsu, A., Lui, S., Weinfurter, A., Chan, S., Hale, T., Clapper,  
665 A., Chang, A., and Höhne, N.: Beyond national climate action: the impact of region, city, and  
666 business commitments on global greenhouse gas emissions, *Climate Policy*, 20, 275-291,  
667 10.1080/14693062.2020.1740150, 2020.
- 668 Melchiorri, M.: The global human settlement layer sets a new standard for global urban data  
669 reporting with the urban centre database, 10, 10.3389/fenvs.2022.1003862, 2022.
- 670 NOAA: Visible Infrared Imaging Radiometer Suite (VIIRS),  
671 <https://www.ngdc.noaa.gov/eog/viirs.html>, Latest Access: July 2023, 2017.
- 672 Pesaresi, M. and Politis, P.: GHS-BUILT-S R2023A - GHS built-up surface grid, derived from  
673 Sentinel2 composite and Landsat, multitemporal (1975-2030), European Commission, Joint  
674 Research Centre (JRC), <http://data.europa.eu/89h/9f06f36f-4b11-47ec-abb0-4f8b7b1d72ea>,  
675 doi:10.2905/9F06F36F-4B11-47EC-ABB0-4F8B7B1D72EA, 2023.
- 676 Schiavina, M., Melchiorri, M., and Pesaresi, M.: GHS-SMOD R2023A - GHS settlement  
677 layers, application of the Degree of Urbanisation methodology (stage I) to GHS-POP R2023A  
678 and GHS-BUILT-S R2023A, multitemporal (1975-2030), European Commission, Joint  
679 Research Centre (JRC), PID: [http://data.europa.eu/89h/a0df7a6f-49de-46ea-9bde-  
680 563437a6e2ba](http://data.europa.eu/89h/a0df7a6f-49de-46ea-9bde-563437a6e2ba), doi:10.2905/A0DF7A6F-49DE-46EA-9BDE-563437A6E2BA, 2023a.
- 681 Schiavina, M., Freire, S., Carioli, A., and MacManus, K.: GHS-POP R2023A - GHS population  
682 grid multitemporal (1975-2030). European Commission, Joint Research Centre (JRC),  
683 <http://data.europa.eu/89h/2ff68a52-5b5b-4a22-8f40-c41da8332cfe>, doi:10.2905/2FF68A52-  
684 5B5B-4A22-8F40-C41DA8332CFE, 2023b.
- 685 Spinoni, J., Vogt, J. V., Barbosa, P., Dosio, A., McCormick, N., Bigano, A., and Füssler, H. M.  
686 J. I. J. o. C.: Changes of heating and cooling degree-days in Europe from 1981 to 2100, 38,  
687 e191-e208, <https://doi.org/10.1002/joc.5362>, 2018.
- 688 Thunis, P., Kuenen, J., Pisoni, E., Bessagnet, B., Banja, M., Gawuc, L., Szymankiewicz, K.,  
689 Guizardi, D., Crippa, M., Lopez-Aparicio, S., Guevara, M., De Meij, A., Schindlbacher, S.,  
690 and Clappier, A.: Emission ensemble approach to improve the development of multi-scale  
691 emission inventories, *EGUsphere*, 2023, 1-27, 10.5194/egusphere-2023-1257, 2023.
- 692 US EIA: US Coal mines, <https://atlas.eia.gov/datasets/eia::coal-mines-1/explore>, 2022a.
- 693 US EIA: US Energy Atlas, [https://atlas.eia.gov/datasets/eia::power-  
694 plants/explore?location=41.629235%2C-118.496000%2C3.79](https://atlas.eia.gov/datasets/eia::power-plants/explore?location=41.629235%2C-118.496000%2C3.79), 2022b.
- 695 USGS: USGS Mineral Resources On-Line Spatial Data, <http://mrdata.usgs.gov/>, Last Access:  
696 January 2019, 2019.





- 697 Van Damme, M., Clarisse, L., Whitburn, S., Hadji-Lazaro, J., Hurtmans, D., Clerbaux, C., and  
698 Coheur, P.-F.: Industrial and agricultural ammonia point sources exposed, *Nature*, 564, 99-103,  
699 10.1038/s41586-018-0747-1, 2018.
- 700 World Bank: Global Gas Flaring Tracker Report, Last  
701 <https://www.worldbank.org/en/programs/gasflaringreduction/global-flaring-data>,  
702 Access: August 2023, 2023.
- 703 World Resources Institute: Global Power Plant Database, Global Energy Observatory, Google,  
704 KTH Royal Institute of Technology in Stockholm, Enipedia, 2018.
- 705 WRI: Global Power Plant Database v1.3.0,  
706 <https://datasets.wri.org/dataset/globalpowerplantdatabase>, 2021.
- 707 Zhang, X., Geng, Y., Shao, S., Dong, H., Wu, R., Yao, T., and Song, J.: How to achieve China's  
708 CO<sub>2</sub> emission reduction targets by provincial efforts? – An analysis based on generalized  
709 Divisia index and dynamic scenario simulation, *Renewable and Sustainable Energy Reviews*,  
710 127, 109892, <https://doi.org/10.1016/j.rser.2020.109892>, 2020.
- 711



**Table 1 – Overview of updated spatial proxies in EDGARv8.0, including data sources and methods.**

Sector and spatial coverage	OLD EDGAR proxies	NEW EDGAR proxies	Details NEW EDGAR proxies	Time coverage	Data access
Power plants (global)	CARMAv3 (not anymore available): 2004, 2009, 2014, fuel type derived from plant capacity (assumption)	Global coal/gas plant tracker (Global Energy Monitor)	Coal, Gas	1970-2050	<a href="https://globalenergymonitor.org/projects/global-coal-plant-tracker/">https://globalenergymonitor.org/projects/global-coal-plant-tracker/</a> and <a href="https://globalenergymonitor.org/projects/global-gas-plant-tracker/">https://globalenergymonitor.org/projects/global-gas-plant-tracker/</a> (2022)
		Global Power Plant Database v1.3.0	Biomass, Other, Oil		<a href="https://datasets.wri.org/dataset/globalpowerplantdatabase">https://datasets.wri.org/dataset/globalpowerplantdatabase</a>
		US EIA	USA power plants, all fuels	All	<a href="https://atlas.eia.gov/datasets/eia::power-plants/explore?location=41.629235%2C-118.496000%2C3.79">https://atlas.eia.gov/datasets/eia::power-plants/explore?location=41.629235%2C-118.496000%2C3.79</a>
		CARMAv3	Autoproducers, countries	2004, 2009, 2014	<a href="http://carma.org/">http://carma.org/</a>
All other industries (Europe)	EPRTR v4*	European Pollutant Release and Transfer Register (EPRTR), v18	All industries and waste plants (with the exception of power plants, iron and steel and coal mines)	2007-2017	<a href="https://www.eea.europa.eu/data-and-maps/data/member-states-reporting-art-7-under-the-european-pollutant-release-and-transfer-register-e-prtr-regulation-23/european-pollutant-release-and-transfer-register-e-prtr-data-base/eptr_v9_csv.zip">https://www.eea.europa.eu/data-and-maps/data/member-states-reporting-art-7-under-the-european-pollutant-release-and-transfer-register-e-prtr-regulation-23/european-pollutant-release-and-transfer-register-e-prtr-data-base/eptr_v9_csv.zip</a>
Iron and Steel (global)	In-house EDGAR	Global steel plant tracker (Global Energy Monitor)		1970-2050	<a href="https://globalenergymonitor.org/projects/global-steel-plant-tracker/">https://globalenergymonitor.org/projects/global-steel-plant-tracker/</a>



Coal mines (global)	USGS derived proxies, Global Energy Observatory (China)	Global coal mine tracker (Global Energy Monitor)	Brown and hard coal, surface and underground	1970-2050	<a href="https://globalenergymonitor.org/projects/global-coal-mine-tracker/">https://globalenergymonitor.org/projects/global-coal-mine-tracker/</a>
		Global Energy Monitor + EIA (Energy Information Administration)	USA all fuels, more precise open and close years	1970-2050	<a href="https://atlas.eia.gov/datasets/eia::coal-mines-1/explore">https://atlas.eia.gov/datasets/eia::coal-mines-1/explore</a>
		EDGAR old proxy	For missing countries	Key years	
Flaring (global)	NOAA-NDGC (2015) VIIRS data <a href="https://www.ngdc.noaa.gov/eog/viirs.html">https://www.ngdc.noaa.gov/eog/viirs.html</a>	Global Gas Flaring Tracker Report (2023)	Used both for venting and flaring activities	2012-2022	<a href="https://www.worldbank.org/en/programs/gas-flaringreduction/global-flaring-data">https://www.worldbank.org/en/programs/gas-flaringreduction/global-flaring-data</a>
Small scale combustion (global)	Global Human Settlements Layer (1975, 1990, 2000, 2015)	Global Human Settlements Layer data Package 2023 + Heating Degree Days from ERA5	For all fuels	Population every 5 years from 1975 to 2030, HDD every year from 1970 to 2022	<a href="https://ghsl.jrc.ec.europa.eu/ghs_pop2023.php">https://ghsl.jrc.ec.europa.eu/ghs_pop2023.php</a> and <a href="https://cds.climate.copernicus.eu/cdsapp#!/dataset/reanalysis-era5-single-levels?tab=form">https://cds.climate.copernicus.eu/cdsapp#!/dataset/reanalysis-era5-single-levels?tab=form</a>
Small scale combustion in agriculture (global)-Rural population	Global Human Settlements Layer (1975, 1990, 2000, 2015)	Global Human Settlements Layer data Package 2023, including GHS-SMOD R2023A - GHS settlement layers + Heating Degree Days from ERA5	For small-scale combustion in agriculture which are mostly associated to rural areas.	Population every 5 years from 1975 to 2030, HDD every year from 1970 to 2022	<a href="https://ghsl.jrc.ec.europa.eu/ghs_pop2023.php">https://ghsl.jrc.ec.europa.eu/ghs_pop2023.php</a> , <a href="https://ghsl.jrc.ec.europa.eu/ghs_smod2023.php">https://ghsl.jrc.ec.europa.eu/ghs_smod2023.php</a> , and <a href="https://cds.climate.copernicus.eu/cdsapp#!/dataset/reanalysis-era5-single-levels?tab=form">https://cds.climate.copernicus.eu/cdsapp#!/dataset/reanalysis-era5-single-levels?tab=form</a>
Intensive livestock and fertiliser industries (global)	Livestock density maps	ESA World Emission project +intensive livestock point sources were taken from EPRTv18 for Europe.	For intensive livestock and fertiliser industry+ gapfilling with livestock density map	2008-2022	<a href="https://www.world-emission.com/">https://www.world-emission.com/</a>
Gap-filling of industrial activities (global)	Population based	Built-up for non-residential areas from Global Human	It is used entirely when no information is available or attributing a fraction of	every 5 years from 1975	<a href="https://ghsl.jrc.ec.europa.eu/ghs_buS2023.php">https://ghsl.jrc.ec.europa.eu/ghs_buS2023.php</a>



		Settlements data package 2023	emissions which was not allocated to point sources.	to 2030	
<b>International shipping</b>	In-house EDGAR proxy based on LRIT and Wang et al. (2007) and Trombetti et al. (2017)	STEAM (Ship Traffic Emission Assessment Model)	Based on CO2 emissions for multi vessels and multi-years.	2000-2018	Jalkanen et al., 2012; Johansson et al., 2017